

# Physical processes in the vicinity of the cometopause: direct measurements of plasma, magnetic field, and waves by Vega-2

M. I. Verigin, A. A. Galeev, R. Grard, K. I. Gringauz, E. G. Eroshenko, S. I. Klimov, M. É. Mogilevskii, A. P. Remizov, W. Riedler, R. Z. Sagdeev, S. P. Savin, K. Szego, A. Yu. Sokolov, M. Tátrallyay, and K. Schwingenshuh

*Space Research Institute, Academy of Sciences of the USSR, Moscow,  
Institute for Terrestrial Magnetism and Radiowave Propagation, Academy of Sciences of the USSR, Troitsk,  
Space Research Institute, Austrian Academy of Sciences, Graz,  
and Space Physics Division, European Space Agency, Netherlands*

(Submitted April 24, 1987)

Pis'ma Astron. Zh. 13, 907-916 (October 1987)

In this article, we analyze the physical processes in the vicinity of the cometopause. We use simultaneous measurements of plasma, magnetic field, and waves by the Vega-2 spacecraft. Large-scale variations in the plasma flux and in the magnetic field are an indication that the fire-hose instability has developed near the cometopause, leading to pitch-angle scattering and deceleration of the proton flux. As a result, charge exchange becomes an efficient mechanism for enhancing the loading of the plasma flux. There is an increase in the intensity of plasma waves in the lower hybrid frequency range. This leads to acceleration of superthermal electrons, and to the excitation of high-frequency oblique Langmuir waves.

**Introduction.** Plasma measurements were performed by means of the PLAZMAG-1 instrument on board the Vega spacecraft in the vicinity of Comet Halley. These measurements have discovered a sharp boundary (a cometopause) behind the shock front at distances of  $\approx 1.6 \cdot 10^5$  km from the nucleus. This boundary separates the region which is controlled by the flow of protons in the solar wind from the region of cometary plasma. The latter consists predominantly of slowly moving heavy cometary ions.<sup>1-4</sup> The existence of this boundary in the space around the comet has also been confirmed from data from the APV-H wave experiment<sup>5</sup> on Vega-1 and Vega-2, as well as by the experiments PICCA and JPA on the Giotto spacecraft.<sup>6,7</sup>

It is true that indications of passing through the cometopause can be found in the published data from many of the experiments on board Vega-1, Vega-2, and Giotto (see, e.g., Refs. 2 and 3). Nevertheless, there does not yet exist a description of the ensemble of phenomena which occur in the vicinity of the cometopause, based on a combined consideration of simultaneous plasma, magnetic, and wave measurements. Moreover, a theoretical analysis of the physical mechanisms which are responsible for the formation of a cometopause is also lacking. In the present paper, we attempt to analyze the physical processes in the vicinity of the cometopause on the basis of data from Vega-2: the data which we discuss include simultaneous measurements of plasma, magnetic field, and waves, in the vicinity of the cometopause.

**Experimental data.** Measurements of the energy spectra of the ion and electron components of the plasma were performed on the Vega-2 spacecraft using the PLAZMAG-1 complex.<sup>2</sup> Included in this complex was a cometary ion analyzer (CA), oriented in the direction of the vector velocity of the spacecraft relative to the comet. This instrument recorded ions with energy per charge in the range 15-3500 eV/Q. An analyzer was also oriented in the direction of the sun. This analyzer (SA) measured the flux of ions in the range 50-25,000 eV/Q. An electrostatic analyzer (EA) was oriented perpendicular to the plane of the ecliptic, and measured the energy spectra of electrons in the range 3-10,000 eV.

The magnetic field was measured<sup>8</sup> by means of a three-component ferrosonde magnetometer (MISHA).

The range was  $\pm 100$  nT in each component, with a resolution of 0.05 nT.

The intensity of plasma waves was measured on Vega-2 by means of two instruments<sup>9,10</sup>: APV-N and APV-V. The first of these was used to measure the amplitude of the oscillations in one of the components of the electric field, and the amplitude of the fluctuations in the ion flux in the direction of the vector velocity of the spacecraft relative to the comet in the frequency range 0.01-1000 Hz. The APV-V instrument was used to measure the amplitude of the same component of the electric field in the frequency range 0-300 kHz.

In the upper part of Fig. 1 we present a spectrogram of the ion fluxes which were measured by the CA analyzer of the PLAZMAG-1 instrument in the vicinity of the magnetopause. The outermost contours in this figure correspond to a counting rate of  $10^3$  sec<sup>-1</sup> in the CA analyzer. Each successive inner contour corresponds to an increase in the counting rate of this analyzer by a factor of 2. The vertical dashed lines in Fig. 1 denote the time interval when Vega-2 passed through the cometopause<sup>1</sup>: 6.43-6.45 UT.

From the spectrogram presented in Fig. 1, there is a noticeable increase in the mean value of the energy per charge of the ions recorded by the CA analyzer in the vicinity of the cometopause: the increase is from  $\approx 170$  to  $\approx 900$  V. This increase is obviously associated with the change in the velocity distribution function and the mass composition of the plasma in the vicinity of the cometopause. As a result of this change, the protons which predominate in the cometsheath ( $m = 1$ ) are replaced by ions in the water group ( $M \approx 16-18$ ). There is a noticeable reduction in the flux of protons recorded by the CA analyzer after the cometopause. However, at the same time, their energy spectra become broader,<sup>1</sup> and the mean energy increases to  $\approx 250$  eV.

In front of the cometopause, the energy spectra of the ions recorded by the SA analyzer have two maxima. (See Fig. 1c in Ref. 1.) The first maximum is composed mainly of protons, and has a mean energy of  $\approx 300$  eV. In the second maximum, the ions belong to the water group, and have typical energies of  $\approx 900$  eV. After passing through the

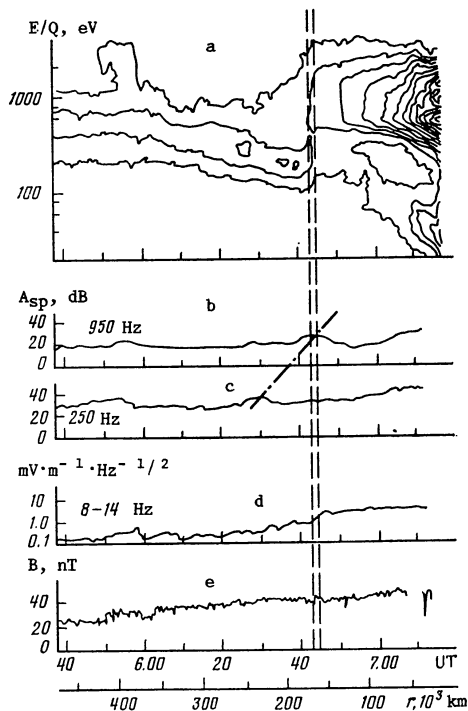


FIG. 1. (a) Spectrogram of ion fluxes; (b), (c) spectral amplitude ( $A_{sp}$ ) of the fluctuations in ion flux; (d) spectral amplitude of the electric field (e) absolute magnitude of the magnetic field. Data from measurements on Vega-2. All quantities are shown in the vicinity of the cometopause (vertical dashed lines). The dot-dashed line denotes the increase in frequency of oblique Langmuir waves around this boundary.

cometopause, there are practically no protons recorded in the direction of the SA analyzer. And the mean energy of the heavy ions stays practically unchanged.<sup>1</sup>

The energy spectra of electrons measured by EA undergo no essential variation as Vega-2 passes through the cometopause.<sup>1</sup> Consequently, there are no variations in the plasma density or in the electron temperature.

Magnetic field measurements which were made in the vicinity of the cometopause by means of the MISHA magnetometer also indicate that there are no substantial changes in the plasma density as Vega-2 passed through this boundary. The absolute magnitude of the magnetic field was practically invariant in the vicinity of the cometopause (see the measurements in the lower part of Fig. 1). And in the  $B_x$  and  $B_y$  components of the magnetic field, only insignificant changes were observed.<sup>1,8</sup>

In the middle part of Fig. 1 we show the results of measuring the wave activity by means of the detectors APV-N and APV-V on Vega-2. On the whole, for the spectral intervals presented in Fig. 1 (and for other intervals also), there is a characteristic increase in the mean amplitude of the oscillations in the plasma flux and the electric field as Vega-2 approaches the nucleus. This increase sets in at a distance of  $(1.5-2) \cdot 10^5$  km from the nucleus. Moreover, in the vicinity of the cometopause (6.30-6.50 UT), oscillations in the plasma flux are recorded in the whistler frequency range (0.2-1 kHz). And for a period of  $\approx 2$  min, a rapid increase was seen in the amplitude of electric field oscillations in the lower hybrid frequency range (8-14 kHz).

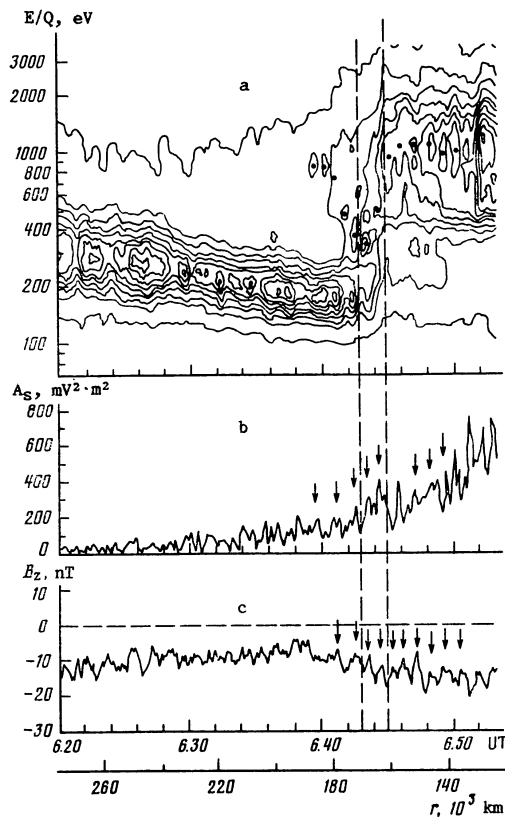


FIG. 2. (a) Detailed spectrogram of the ion fluxes; (b) amplitude of electric field oscillations,  $A_e$ ; (c)  $B_z$  component of the magnetic field. All quantities refer to the vicinity of the cometopause. Filled circles denote local maxima in the ion flux. Arrows denote the corresponding maxima in the lower hybrid oscillations in the electric field and in the  $B_z$  component of the magnetic field.

Wave activity is also present in the region of the cometopause at lower frequencies. This conclusion can be drawn from the more detailed measurements of plasma, magnetic field, and waves which are shown in Fig. 2. In this figure, contours are constructed on the spectrogram from the CA analyzer with an increment of  $440 \text{ sec}^{-1}$ . (The outermost contour corresponds to a counting rate of  $10^3 \text{ sec}^{-1}$ .) During the ten minute interval in the vicinity of the cometopause, the filled circles on the spectrogram denote the times when local maxima were observed in the ion flux. We can compare simultaneous spectrograms from the CA and SA analyzers (see, e.g., Fig. 1 in Ref. 1, where these spectrograms have been presented in color-coded form.) This shows that changes in the ion fluxes entering these two analyzers occur in antiphase. This result can be considered as evidence for the presence of large-scale MHD variations in the direction and/or the velocity of the plasma flow in the vicinity of the cometopause. These variations have a characteristic period  $T \approx 1$  min.

Large-scale MHD variations in the plasma flux in the vicinity of the cometopause also manifest themselves elsewhere in that data in Fig. 2. They can be seen in the amplitude of the oscillations in the electric field in the lower hybrid frequency range (2-32 Hz), as well as in the variations in the  $B_z$  component of the magnetic field. The characteristic time for these is  $\approx 1$  min. The arrows in Fig. 2 denote maxima in the amplitude of lower hybrid oscil-

lations and in the  $B_z$  component corresponding to the maxima in the ion fluxes.

**Discussion.** There is a rapid decrease in the flux of protons in both of the analyzers, i.e., in the direction of the comet and in the direction of the sun (Fig. 2). (By "rapid" we mean a duration of  $\approx 2$  min, over a length of  $\Delta \approx 10^4$  km along the trajectory of Vega-2.) It is impossible to explain this rapid decrease without relying on collisionless mechanisms of deceleration and/or isotropization of the proton distribution due to the development of an instability arising from the relative motion between the solar wind protons and the cometary ions. We will therefore estimate first of all the velocities of the protons and ions which were recorded by the PLAZMAG-1 instrument.

We can obtain a rough estimate of the translational velocity of the protons relative to the spacecraft from the fact that, in front of the cometopause, the mean energy of solar wind protons is  $\approx 300$  eV in the direction towards the sun. We find that the relative proton velocity is  $V_{pr} \approx 250$  cm/sec. The velocity of the protons relative to the comet is  $V_p \approx 200$  km/sec: this can be derived by vector subtraction of the velocity of the spacecraft relative to the comet ( $V_{sc} \approx 80$  km/sec). A possible vector diagram for these various velocities are shown in Fig. 3 in a coordinate system fixed in the spacecraft. Also shown are the sector fields of view of the CA and SA analyzers. Vertical hatching denotes the possible regions in velocity space from which protons were incident on these analyzers. In an analogous way, we can estimate the velocity of the heavy cometary ions relative to the spacecraft ( $V_{ir} \approx 120$  km/sec) and relative to the comet ( $V_i \approx 60$  km/sec).

According to the measurements, the magnetic field points almost directly along the flow. Therefore we would expect the hydrodynamic fire-hose instability to develop. However, with the proton density and magnetic field strength that are present in front of the cometopause ( $n_p \approx 10\text{--}20$  cm $^{-3}$ ,  $B \approx 40$  nT), the conditions for the development of the fire-hose instability are not satisfied in the flow of the solar wind relative to the cometary plasma. On the other hand, since the density of heavy ions is  $n_i \approx 10$  cm $^{-3}$ , and their velocity relative to the comet is  $V_i \approx 60$  km/sec, the ionization of a comparable quantity of cometary gas leads to instability in the motion of protons and cometary ions relative to the ionized atoms in the cometary gas. As a consequence, the protons are decelerated, and they undergo pitch-angle scattering. This leads to the fall-off in the intensity of the ion flux which was recorded by the CA and SA analyzers.

An unambiguous sign of the development of instability near the cometopause is the presence of large-scale variations in plasma flux correlated with oscillations in the magnetic field components transverse to the main field (Fig. 2). The characteristic scale-length of these oscillations along the spacecraft trajectory ( $\delta \approx V_{sc}$ ,  $T \approx 5000$  km) is comparable to the scale-length of the cometopause ( $\Delta$ ), but it is much larger than the Larmor radius of the cometary ions:  $\rho_{ci} \approx V_i/\omega_{ci} \approx 300$  km. (Here,  $\omega_{ci} \approx 0.2$  sec $^{-1}$  is the cyclotron frequency of the ions in the water group.) In the absence of measurements of the oscillations in the vector velocity of the plasma, it is impossible to establish the type of oscillations which are excited as a result of the instability. However, the fact that the modulus of the magnetic field is constant implies that the oscillations are transverse.

The amplitude of the oscillation in velocity,  $\delta V_{\perp}$ , can be evaluated on the basis of the magnitude of the amplitude of the oscillations in the transverse components of the magnetic field,  $\delta B_{\perp}$ :

$$\delta V_{\perp} \approx V_A \frac{\delta B_{\perp}}{B} \approx 10 \text{ km/sec.} \quad (1)$$

Here,  $V_A \approx 60$  km/sec is the Alfvén velocity that is sufficient to create a large modulation of the ion fluxes in both analyzers. At the same time, the fact that the length scale of these oscillations is large compared with the Larmor radius of the ions shows that they are excited in a nonresonant manner. In other words, we seem to be observing the development of a fire-hose instability with a growth-rate which is significantly greater than the growth-rate of the resonant instability. The source of energy for this instability is the kinetic energy of the cometary ions that have been created in the plasma flow relative to that flow: this has a density which is significantly larger than the density of protons in the solar wind.

The significant reduction in the proton flux in the vicinity of the cometopause and also in the heart of the cometary plasma indicates that cometary ions are being formed by an additional effective mechanism: this is charge exchange between the protons and the cometary gas. As a result, there is an increase in the rate of plasma loading in this region. In order to estimate the characteristic time for charge exchange,  $\tau_{ct}$ , we need to make use of the total velocity of the protons:

$$\tau_{ct} \approx (\sigma_{ct} V_p n_n)^{-1} \approx 6 \cdot 10^3 \text{ sec.} \quad (2)$$

Here,  $\sigma_{ct} \approx 2 \cdot 10^{-15}$  cm $^2$  is the charge exchange cross-section;  $n_n \approx 4 \cdot 10^3$  cm $^{-3}$  is the density of neutral gas near the cometopause, at cometocentric distances of  $R \approx 1.6 \cdot 10^5$  km (see Ref. 11); and  $V_p \approx 200$  km/sec is the velocity with which the protons pass through the cometopause. The latter is equal (within an order of magnitude) to the velocity of their gyrorotation at the cometopause and behind it due to pitch-angle scattering by the oscillations which have been excited. The time estimated above,  $\tau_{ct}$ , is comparable to the characteristic time

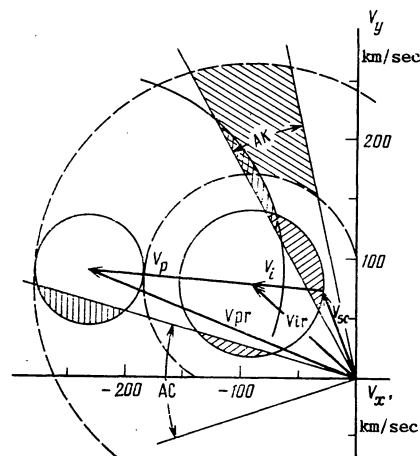


FIG. 3. Qualitative vector diagram of the velocities of the proton and ion components of the plasma flow in the vicinity of the cometopause. We show the velocities relative to the comet ( $V_p$ ,  $V_i$ ), relative to the spacecraft ( $V_{pr}$ ,  $V_{ir}$ ), and velocities relative to the spacecraft of ions which are flowing in a coordinate system attached to the comet ( $V_{sc}$ ).

required for the plasma flow to flow past the comet in the vicinity of the cometopause ( $\approx 2R/V_i \approx 5 \cdot 10^3$  sec), using the hydrodynamic velocity of the flow ( $V_i \approx 60$  km/sec). This indicates that charge exchange is indeed effective in this region.

A consequence of the presence of a beam of cometary ions in the plasma flow is that the intensity of plasma waves near the cometopause increases in the lower hybrid frequency range (Fig. 3). These waves grow until quasilinear relaxation reduces the ion beams to a stable state in which the wave intensity is of order<sup>12</sup>:

$$E^2 \approx \frac{n_n M^2 V_p^2}{\tau_i n_p e^2} \approx 1 \text{ mV}^2 \cdot \text{m}^{-2} \cdot \text{Hz}^{-1}, \quad (3)$$

Here,  $E^2/8\pi$  is the spectral energy density of the electric field of the lower hybrid oscillations; and  $\tau_i \approx 5 \cdot 10^5$  sec is the characteristic time required for the neutral gas to be ionized (allowing for the effects discussed above concerning the enhanced efficiency of charge exchange in the vicinity of the cometopause). The intensity of lower hybrid waves measured in this region by the instruments APV-V (Fig. 1) and APV-N (Fig. 2) are found to agree reasonably well with the theoretical estimate in (3).

Once the lower hybrid waves are excited, they in turn will accelerate superthermal electrons which happen to be in Cherenkov resonance with them (Refs. 13, 14). If the lifetime of the superthermal electrons is significantly longer than the acceleration time-scale, then the maximum density of these electrons,  $n_{Te}$ , will be determined by the condition that the electron Landau damping is small compared to the growth rate of the instability. In that case, the efficiency of energy transfer from ions in the beam (with density  $n_b \approx n_i$ ) turns out to be of order unity. (The factor  $\eta \approx 7.5\%$  is the efficiency of energy transfer by the electrons.) Hence, the density  $n_{Te}$  and energy  $\epsilon_e$  of the superthermal electrons may be estimated as<sup>13</sup>:

$$n_{Te} \approx n_b \approx 1 \text{ cm}^{-3}, \quad \epsilon_e \approx MV_i^2/2 \approx 300 \text{ eV}. \quad (4)$$

The superthermal electron density, which is estimated from Eq. (4), agrees with direct measurements.<sup>15</sup> However, it is not enough to explain the observed growth in the density of cometary ions by means of electron collisions.

When superthermal electrons are accelerated along the magnetic field lines, oblique Langmuir waves are excited in the plasma. (If the plasma has high  $\beta$ , the waves will be whistlers.) The reason is that the electron velocity distribution is anisotropic. The frequency at which the intensity of these waves reaches a maximum is approximately equal to

$$\bar{\omega} \approx \omega_{ce} v_{Te} / (\epsilon_e / m_e)^{1/2} \approx 2.3 \cdot 10^3 \text{ sec}. \quad (5)$$

Here,  $\omega_{ce} \approx 7 \cdot 10^3 \text{ sec}^{-1}$  is the electron cyclotron frequency, and  $v_{Te} \approx 2.5 \cdot 10^8 \text{ cm/sec}$  is the thermal velocity of the electrons corresponding to their temperature in the vicinity of the cometopause ( $\approx 2 \cdot 10^5 \text{ K}$ ; see Ref. 4). Taking into consideration the nonlinear limitation on the amplitude of the high-frequency Langmuir waves, it can be shown<sup>16</sup> that

$$E^2 \approx 4\pi n_{Te} \epsilon_e (\omega_{ce} / \omega_{pe})^2 (\bar{\omega} / \omega_{ce})^5 \approx 20 \text{ mV}^2 \cdot \text{m}^{-2} \cdot \text{Hz}^{-1}, \quad (6)$$

where  $\omega_{pe} \approx 2 \cdot 10^5 \text{ sec}^{-1}$  is the electron plasma frequency. According to Eqs. (3) and (6), and

according to the measurements, the spectral energy density of the oscillations in the electric field in the oblique Langmuir waves is of the same order of magnitude as in the lower hybrid waves. We note that excitation in a plasma of lower hybrid and whistler oscillations with similar energy densities is a typical feature of the interaction between a plasma flow and a gas: this has been discussed previously in an application to the Io torus.<sup>16</sup>

According to Eq. (5), the frequency of the high-frequency Langmuir waves becomes larger as the plasma is decelerated in the vicinity of the cometopause, because the energy of the superthermal electrons is reduced according to Eq. (4). This increase is denoted in Fig. 1 by a sloping dot-dashed line. The enhanced level of lower hybrid and whistler oscillations in the plasma is merely a consequence of the rapid loading of the solar wind by the cometary ions in the vicinity of the cometopause, with the subsequent deceleration, but it is not the reason for it.

- <sup>1</sup>K. I. Gringauz, T. I. Gombosi, M. Tátrallyay, et al., *Geophys. Res. Lett.* **13**, 613 (1986).
- <sup>2</sup>K. I. Gringauz, T. I. Gombosi, A. P. Remizov, et al., *Pis'ma Astron. Zh.* **12**, 666 (1986) [*Sov. Astron. Lett.* **12**, 279 (1986)]; K. I. Gringauz, T. I. Gombosi, A. P. Remizov, et al., *Nature* **321**, 282 (1986); *Adv. Space Res.* **5**, 165 (1985).
- <sup>3</sup>K. I. Gringauz, M. I. Verigin, A. K. Richter, et al., in: *Explorations of Halley's comet*, ESA SP-250 (1986), Vol. 1, p. 93.
- <sup>4</sup>K. I. Gringauz, A. P. Remizov, M. I. Verigin, et al., in: *Explorations of Halley's comet*, ESA SP-250 (1986), Vol. 1, p. 195.
- <sup>5</sup>S. Savin, G. Avanesova, M. Balikhin, et al., in: *Explorations of Halley's comet*, ESA SP-250 (1986), Vol. 3, p. 433.
- <sup>6</sup>A. Korth, A. K. Richter, K. A. Anderson, C. W. Carlson, D. W. Curtis, R. P. Lin, H. Reme, J. A. Sauvaud, C. D'Uston, F. Cotin, A. Cros, and D. A. Mendis, *Adv. Space Res.* **5**, 221 (1986).
- <sup>7</sup>E. Amata, V. Formisano, R. Cerulli-Irelli, et al., in: *Exploration of Halley's comet*, ESA SP-250 (1986), Vol. 1, p. 213.
- <sup>8</sup>W. Riedler, K. Schwingenshuh, E. G. Eroshenko, V. A. Styazhkin, and C. T. Russell, *Pis'ma Astron. Zh.* **12**, 647 (1986) [*Sov. Astron. Lett.* **12**, 272 (1986)]; W. Riedler, K. Schwingenshuh, Ye. G. Yeroshenko, and C. T. Russell, *Nature*, **321**, 288 (1986).
- <sup>9</sup>S. Kimov, S. Savin, Ya. Aleksevich, et al., *Pis'ma Astron. Zh.* **12**, 688 (1986) [*Sov. Astron. Lett.* **12**, 288 (1986)]; S. Klimov, S. Savin, Ya. Aleksevich, et al., *Nature* **321**, 292 (1986).
- <sup>10</sup>R. Grard, K. Begin, M. Mogilevskii, Yu. Mikhailov, O. Molchanov, A. Pedersen, J.-G. Trotignon, and V. Formisano, *Pis'ma Astron. Zh.* **12**, 683 (1986) [*Sov. Astron. Lett.* **12**, 286 (1986)]; R. Grard, A. Pedersen, J.-G. Trotignon, et al., *Nature* **321**, 290 (1986).
- <sup>11</sup>A. P. Remizov, M. I. Verigin, K. I. Gringauz, I. Apathy, I. Szemerey, T. I. Gombosi, and A. K. Richter, in: *Exploration of Halley's Comet*, ESA SP-250 (1986), Vol. 1, p. 387.
- <sup>12</sup>V. Formisano, A. A. Galeev, and R. Z. Sagdeev, *Planet. Space Sci.* **30**, 491 (1982).
- <sup>13</sup>O. L. Vaisberg, A. A. Galeev, G. N. Zastenker, S. I. Klimov, M. N. Nozdrachev, R. Z. Sagdeev, A. Yu. Sokolov, and V. D. Shapiro, *Zh. Eksp. Teor. Fiz.* **85**, 1232 (1983) [*Sov. Phys. JETP* **58**, 716 (1983)].
- <sup>14</sup>A. A. Galeev and I. Kh. Khabibrakhmanov, *Origin and energetics of Io torus*, in: *Giant Planets and their Satellites*, M. G. Kivelson (ed.), Pergamon Press, Oxford (1983), p. 71.
- <sup>15</sup>C. D'Uston, H. Reme, J. A. Sauvaud, et al., in: *Exploration of Halley's comet*, ESA SP-250 (1986), Vol. 1, p. 77.
- <sup>16</sup>A. A. Galeev and I. Kh. Khabibrakhmanov, *Pis'ma Astron. Zh.* **11**, 292 (1985) [*Sov. Astron. Lett.* **11**, 118 (1985)].

Translated by D. J. Mullan

# Nonlinear self-similar problems of nonstationary disk accretion

Yu. É. Lyubarskii and N. I. Shakura

*Institute of Space Research, Academy of Sciences of the USSR, Moscow  
and P. K. Shternberg State Astronomical Institute, Moscow*

(Submitted January 28, 1987)

*Pis'ma Astron. Zh.* 13, 917-928 (October 1987)

Self-similar solutions of the fundamental equation describing nonstationary disk accretion are obtained.

The currently known series of solutions of the gas-dynamic equations describing the time evolution of a flattened disk configuration in an external gravitational field (accretion disks in binary systems, protoplanetary nebulae, galactic disks, etc.) is a limited class of solutions of linear problems of nonstationary disk accretion. In these problems the viscous torque arising between adjacent layers of a differentially rotating disk depends linearly on the surface density, which permits the problem of the evolution of nonstationary disks to be reduced to the solution of a linear differential equation of the diffusion type.<sup>5,10,9</sup> In the more general formulation of the problem, when the fundamental equation of nonstationary disk accretion is a nonlinear partial differential equation, its solutions have been obtained only numerically by computer (see, e.g., Refs. 8, 2, 3).

Widely known similarity methods, which are usually applied to the solution of nonlinear heat transfer and diffusion problems,<sup>7,1</sup> are used below to obtain a series of self-similar solutions of the fundamental equation of nonstationary disk accretion. These solutions, asymptotically exact for real problems, give very important information about the nature of the evolution of nonstationary disks, which does not follow directly from the numerical calculations.

## 1. General Pattern

Qualitative description of nonstationary accretion onto a black hole. Let a gaseous formation, close to a ring in shape, appear at some time at a great distance from a black hole ( $r_0 \gg r_g = 2GN/c^2$ ). This can occur in a binary stellar system due to the short-term ejection of material from the neighboring component. A ring around a supermassive black hole in the nucleus of an active galaxy could form as a result of the tidal disruption of a giant star. When there are effective viscous mechanisms (turbulence of random small-scale magnetic fields), the differentially rotating ring will begin to disperse into a disk.

The process of ring diffusion can be divided into three characteristic stages, and each of these stages is described by a self-similar solution (of type I or II) of the initial nonlinear partial differential equation, i.e., motions arise at each stage whose distinguishing feature is similarity conserved in the motion itself. This means<sup>7</sup> that the distribution of any physical quantity, say, the surface density of material in the disk  $\Sigma$  [g/cm<sup>2</sup>] can be represented as  $\Sigma(r, t) = S(t)s[r/R(t)]$ , where the dimensional scale of the quantity itself  $S(t)$  [g/cm<sup>2</sup>] and the coordinate scale  $R(t)$  depend on time in an arbitrary manner, while the dimensionless ratio  $s[r/R(t)] = s(\xi)$  is a universal function of one self-similar variable  $\xi = r/R(t)$ .

At the first stage, material at the inner edge of the formation, in losing angular momentum to

radially outward layers, begins to move toward the center, and in the region  $r \ll r_0$  the flow evolves into some self-similar mode whose characteristics are independent of the initial mass distribution profile. The inner edge of the disk, which has the form of an expanding "tongue," reaches the accretion center in a finite time (Fig. 1a). The self-similar solution begins to break down near the radius of the last stable orbit; nevertheless, after a short-term transition mode in this region, which is not self-similar, the accretion again evolves into another self-similar solution — the quasistationary accretion mode (the second stage).

At the second stage, quasistationary accretion with a slowly increasing accretion rate, which is practically constant radially, is rapidly established in the inner regions of the disk (in view of the small characteristic times for the course of all the processes at small radii). This region is separated by some transition zone from the outer regions where no changes have yet occurred and the distribution of all the physical quantities must remain the same as that established at the preceding stage. The region of the quasistationary solution will expand as the transition zone advances radially outward (Fig. 1b). After the transition zone reaches the region of the initially ejected material, whose distribution has remained practically constant, since the formation of the "tongue," a nonself-similar ac-

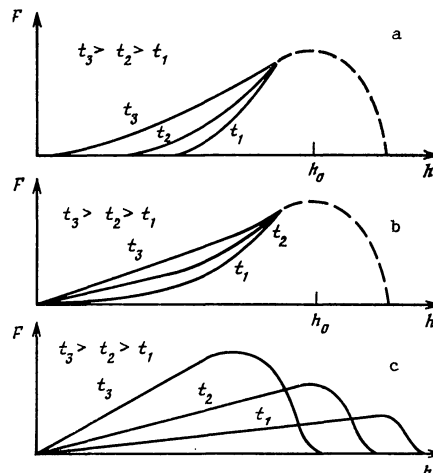


FIG. 1. Qualitative profiles of viscous torques acting between adjacent layers of the disk as a function of the specific angular momentum at the different stages: a) stage of formation and inward motion of self-similar "tongue"; b) stage of formation of quasistationary mode; c) stage of accretion attenuation. Dashes denote the regions into which the material was ejected and in which the solution is nonself-similar;  $t_1 < t_2 < t_3$  denote arbitrary times.